

# SFSA Cast In Steel 2026 – Horseman’s Axe

## Technical Report

Penn State Erie, The Behrend College



**PennState**  
Behrend



Team Name:

We Would Like To Axe You A Question

Team Members:

Steven Fedell, Shawn Foster, Ben Hollerman, Justin Kalgren

Advisor(s) Name:

Dr. Paul C. Lynch and Dr. Chetan Nikhare

Foundry Partner:

Ashland Foundry & Machine Works LLC

## Introduction

Every year the Steel Founders Society of America (SFSA) holds the Cast in Steel competition for groups of university students across North America where teams are tasked with designing and manufacturing a cast product. SFSA has created this competition to encourage students to learn about making steel products using the casting process and applying the latest technology available. This year's competition calls for each group to document their creation of a cast horseman's axe.

A horseman's axe was wielded by soldiers on horseback. It was often used against a variety of armored opponents in battle from the 13<sup>th</sup> to the 15<sup>th</sup> century. It was small and light enough to be swung single-handed while on horseback, but durable enough to withstand striking an opponent's armor. The axe itself was likely based upon the knightly pole axe [1]. These axes evolved from earlier war picks and hammers and would typically consist of a head with an axe blade, top spike, and a hammer or spike on the rear to act as a counterweight [1]. Sometimes, they were equipped with a belt hook or fitted with a hole for a lanyard for ease of carrying. They were able to do damage in a variety of manners, such as swinging, striking, or lunging using the various ends of the axe.

After researching, careful analysis of the desired features, strengths and weaknesses of different variations, and how the casting process affects these features, the team moved forward with several concepts. Once the final design was selected it was iterated upon until a final design was attained. A mold was then designed around the final iteration of the axe. With the utilization of several criteria coming from the advice of industry sponsors and advisors, a mold was designed and printed with phenolic resin chemically bonded sand. This mold was test poured and iterated upon to improve the casting result. With the mold designed and resulting in a successful axe head casting, the axe head was then machined. A haft was carved out of wood based upon the axe-head geometry. Finally, the axe-head and haft were assembled into a fully complete horseman's axe. Note that all pictures, tables, and figures can be found in the Appendix.

## Concept Generation

Historical examples of these axes vary greatly in size, construction, and implementation, in part because they were wielded over several centuries across a very large area [1]. In the past, these axes would have been forged, and this limits the possible geometries that can be manufactured easily. It was decided that due to the weight constraint of 3.3 lbs, the haft of the axe would be made of wood, this allowed more leniency on the design of the head of the axe. Taking these factors into account, various ideas were generated and filtered, leading to three concepts being modelled based upon the aforementioned ideas. These concepts are shown in Figure 1, Figure 2, and Figure 3 of the Appendix. These concepts were ranked based on their historical accuracy, how well they took advantage of the benefits of casting, how much post casting work would be needed to complete the design, weight, and ease of casting. Once the design shown in Figure 3 was selected as a clear winner, it was iterated upon.

## Design Revision

The result of the concept generation and selection process still had unincorporated features that were still desired to be in the final axe. The rough geometries of the head were smoothed out as sharp corners are more prone to casting defects. It was decided that langets should be added to make the axe more structurally sound. Historical examples of axes with langets typically had them stretching the entire length of the haft. This was undesirable, as long thin structures like these are very difficult to cast without significant defects. It was decided that shorter, thicker langets should be implemented in order to cast the head in one piece. This is one advantage of the casting process over that of a traditionally hand forged horseman's axe head, which were usually assembled in multiple pieces. The historical features on this final design include the hammer on the rear, a pick on top, and the axe blade, with langets completing the assembly, as shown in Figure 4. With the final axe head geometry finished, a handle or haft could be designed for a proper fit to the head.

The haft design was based upon the geometry of the head. It would be designed to be inserted into the head, keeping constant geometry through the langets. Upon consideration, it was deemed the haft should gradually taper to the portion where it would be held, to feel better when using it and to add more material for increased strength. The haft shape straightens where it is held and has a swell at the base to prevent the haft from slipping out of the hand that is wielding it. It is also fitted with a lanyard hole, as originally recommended by SFSA [2]. The final haft design is shown in Figure 5.

The final, complete axe design is complete with the haft and the head. These parts are joined via three brass pins. Two of these pins are circular, and the third a rounded square. The full design assembly can be seen in Figure 6.

## Materials Selection

Through research, it was found that modern axes, such as those meeting the standards of the American Red Cross / Red Crescent fireman's axe, should range in hardness between 48 and 57 Rockwell C [3]. Using this standard, steel alloys were filtered to those that could easily be hardened to within this range. This is supported conceptually by the fact that if the steel is too hard it will lose ductility and shatter on impact, and if it is too soft the head will deform too much to retain function. For this reason, the alloy 4340 steel was chosen as the most desirable choice. It is a high strength low alloy steel that is resistant to impact and can be easily heat treated to a desired hardness [4]. Due to availability through the foundry partner, other alloys were considered, and a test pour of 17-4 PH stainless was completed, with the goal of determining potential defects that may arise in the mold design that simulations may not have predicted. The reason this alloy was not poured beyond this test is it must be properly precipitation hardened to achieve the hardness range, as well as other properties of stainless steel that made it more difficult to achieve desired properties than with high strength low alloy steels, such as 4340. After a defective 17-4 PH pour, a pour of 4340 was completed through the

industry partner's investment casting facility. This allowed for a small batch run (i.e. small induction heat) to be carried out.

As previously stated, the decision that the haft of the axe would be made of wood was made early on. After researching a variety of available species of hardwoods, it was decided the haft would be made of white ash. Current axe handles are typically made of either hickory or ash wood. Ash was chosen here due to its ductility and versatility, as it is used in a variety of applications, including baseball bats, and of course hand tools [5]. Historically, ash was also widely available in Europe, thus making it an obvious choice for historical accuracy [6].

## **Non-Destructive Testing**

### **Finite Element Analysis (FEA)**

To ensure the axe's design was one of structural integrity, Ansys Mechanical was used to determine the stresses on the axe for the worst-case scenario. Thus, a large block was added to the CAD model of the axe and imported into Ansys workbench as seen in Figure 7. To properly model the impact situation, the explicit dynamics model was used. This model takes an input of an incoming velocity and incrementally balances the energy involved to find the resulting stresses, deformation, and strain. To determine the initial velocity condition, a mockup of a similarly sized steel hammer was swung at an anvil and videoed. One test of the hammer and video setup is shown in Figure 8. Using the framerate and the movement of the snapshots, the hammer was determined to be moving at 508.57in/s immediately before impact.

In addition to the initial velocity condition, the material properties for the 4340-steel axe and the white ash handle were researched and used to populate the data in Ansys' workbench [7] [8]. Once the data was entered, the model was meshed and the simulation was run to perform a mesh convergence, such that with a 15% increase in elements, there is less than 5% change in maximum stress and less than 1% change in total deflection, as has become an unofficial standard in industry for non-linear models. This mesh convergence was summarized in Table 1. Along the way, and to better determine the stress, there were changes in the integration end time to better match when the maximum stress was being experienced by the blade. The time that was settled on was  $5 \times 10^{-5}$  seconds after impact, which yielded an equivalent Von Mises stress of 226.91ksi as shown in Figure 9 and Figure 10. From Granta, the yield strength of 4340 steel tempered at 315°F is 207 to 254ksi and the Ultimate Tensile Strength (UTS) is between 225 and 289ksi. Even though the maximum stress on the blade does yield and possibly exceed the lowest possible UTS, it was determined this was a success due to the worst-case nature of the setup. Although it is possible the competition will use an anvil-like chopping challenge, the more likely scenario is the challenge would include chopping a material that is softer or yields more than a fixed block of steel. Even if the axe is used against an anvil-like setup, the FEA results provide evidence the edge may yield, but would most likely not fracture, and if fracture occurs, it will be very localized, as shown in Figure 10.

## Hardness Testing

Rockwell C hardness testing was performed on the completed axe head after it was hardened and tempered [9]. The location of the test was on the flat center portion of the head. The result of the testing was a hardness between 48.6 and 49.02 Rockwell C which were within the desired range of 48-57 Rockwell C.

## Mold Design

Given the nature of the competition, a well-designed mold was crucial to ensure the castings would be free of defects. The primary defect concern in the initial design phase was density of the casting, and the secondary concern was the formation of oxides as the mold was filled. Having a fully dense part with as few inclusions as possible would give the axe the best chance of surviving the competition. To that end, the software SOLIDCast 9 was used to simulate molten steel flowing into a variety of mold designs. Given these simulations, relevant information regarding the two primary defect concerns could be extracted. For the first concern, SOLIDCast could directly predict what the density of the axe should be. This made it possible to rapidly iterate on the design to ensure the axe would not have any low-density areas or voids. Reducing the amount of oxides formed was not as straightforward as improving the density. During the team's research, a paper [10] was found that indicated that reducing the amount of turbulent flow in the molten metal would reduce the number of oxides that form. This is because more turbulence in the mold causes more of the highly reactive molten metal to be exposed to the atmosphere, leading to the formation of said oxides. That research paper [10] indicated that achieving a Reynold's number (a dimensionless value that indicates the amount of turbulence) of less than 20,000 was ideal to reduce the formation of oxides in molten steel. This value was calculated by using an average velocity of the molten metal, from the SOLIDCast simulation, along with the dimensions of the of the mold where the associated velocity was taken from. The very first mold design (Mold 1), as seen in Figure 11, was a very simple gating system attached to a slightly oversized model of the axe. The oversized axe model helped to account for any shrinkage that may occur while the part cooled and left extra stock so the axe could be machined during post processing. This oversized model was used for all subsequent mold iterations. This design was then simulated with SOLIDCast which indicated there were issues with part density as seen in an iso-surface plot of material density in Figure 12. The locations the model is colored indicate an area with density below 100%. The entirety of the top spike was below 100% density to varying degrees, which led to revisions being made. Several changes were made to this design over many iterations which led to Mold 1.6, pictured in Figure 14. This mold features an expanded gating system, which includes several more risers. The other major features to note are a connection from the fill sprue to the head of the axe and an additional reservoir for molten metal to fill directly across from it. Both features help to feed molten metal to the axe head as liquid to solid shrinkage occurs as the axe cools down. With the inclusion of those features, it led to the simulation indicating the axe head would be fully dense as seen in Figure 14. Also, a velocity was taken at the top and bottom gates connecting to the axe; a Reynold's number of 16,127 and 29,902 were found for these two areas respectively. While these numbers were not

ideal, they were within the same order of magnitude as the ideal and so this was deemed acceptable as it was a secondary concern. The mold design was then turned into a casting ready mold using 3-D printed phenolic resin chemically bonded sand. Two of these molds were printed and it was early enough that they could be test poured in steel to validate the mold design. These two test pours revealed there were problems with the mold design resulting in hot tearing around the top spike on both pours pictured in Figure 16. This issue resulted in the team learning more about potential causes of hot tearing and led to re-examining the design of Mold 1.6. One important plot that had been previously overlooked during the initial design phase of the mold was the Niyama Criterion. The Niyama Criterion essentially indicates areas where shrinkage defects potentially may occur, and typically, the higher the value of the Niyama Criterion the less chance of a defect. In the case of SOLIDCast and the units it uses, the critical Niyama Criterion value for steel is around 0.2. As previously mentioned, the team reexamined the SOLIDCast simulation of Mold 1.6, specifically looking at the plot of Niyama Criterion. The simulation indicated a potential issue near where the head of the axe transitioned into the top spike, as seen in Figure 15. In the case of the test axes, this shrinkage likely resulted in the hot tearing seen very near to where the simulation predicted Niyama Criterion value of around 0.042, nearly five times lower than the critical value. This discovery led to a complete redesign of the axe and several more iterations resulted in Mold 2.9, seen in Figure 17. While this mold still featured the oversized axe model, everything else had been changed; the gating system had been vastly simplified and a significantly larger reservoir for molten metal was added. All of these changes were made in order to increase the value of the Niyama Criterion (i.e. a lower risk of defects) predicted by SOLIDCast while still ensuring it also predicted the finished product would be 100% dense; this can be seen in Figure 19 and Figure 18 respectively. Once again, the Reynold's number was calculated for both the top and bottom gates, with a value of 44,290 and 23,465 respectively. Once again, these values were higher than the ideal value of 20,000 or less. However, they remained within the same order of magnitude, and considering the delicate balancing that took place in order to increase material density while maintaining an acceptable Niyama Criterion value, this was once again deemed acceptable.

## Haft Carving

The haft started as 3"x3"x37" white ash baseball bat blanks. These blanks, chosen for their straight grains, were ideal for carving the haft. The blank was turned on a manual lathe, shown in Figure 20, allowing for the implementation of a smooth, consistent taper. Once it was turned to an appropriate radius, a belt sander was used to shape the flat sides, as shown in Figure 21. The haft was then hand sanded to a smooth, desired finish to ensure a proper fit with the axe-head, and boiled linseed oil was applied to the wood to seal it before assembly.

## **Machining, Heat Treatment, and Finishing Processes**

After the successful casting of four axes, one of which can be seen in Figure 22, the gating system was removed and the axes were sent off to be HIPed (Hot Isostatic Pressing). The castings were put in a pressure vessel and heated to 1200°C at 15 ksi of pressure for four hours. This process helped to close off any microporosity that formed during the casting of the axes, which helps to increase the ductility and strength of the axe. Once back from being HIPed, post processing was started on the axe with the first process being machining. The axe was put into a CNC machine, and it was milled flat as pictured in Figure 23. This established a reference surface that could be used to ensure the following machining operations were located correctly. The initial profile was machined into the axe using 2-D tool paths before the more complex geometry could be milled using 3-D tool paths as seen in Figure 24. After machining was finished, the axe was heat treated by putting into a furnace at 900°C for 1 hour before being quenched in a 20% polymer solution. The polymer in the quenchant serves to slow down the heat transfer rate between the axe and the quenchant to decrease the probability of quench cracking. The axe was then tempered immediately after quenching in another furnace for 3 hours at 250°C to achieve the desired hardness. The axe after this process can be seen in Figure 25. Next, the axe was sharpened and polished. Figure 26 shows the axe with a rough edge during the polishing stage after sanding with 180 grit paper. Polishing was completed down to 320 grit that was then finished with Scotch Brite and then the axe was sharpened as seen in Figure 27. The pins were then machined out of brass to fit the axe head, and corresponding holes were drilled into the haft. The axe head and haft were fitted together, and a small amount of epoxy was then applied to the pin holes before the pins were inserted and panned over to ensure a tight fit. The pins were then filed and sanded flush with the axe head and the blade was oiled to prevent rust formation before the competition. The finished axe can be seen in Figure 28, the final weight of the axe is 2.8 lbs and the final length is 30.5 inches.

## **Conclusion**

The final axe met the competition requirements and is within the 31.5 inch length and 3.3 pound weight limits. It resembles other horseman's axes that have been developed throughout history, complete with langets, a top spike, a war hammer, and of course, a blade. The axe head fell within the desired hardness range of 48-57 Rockwell C, with final values between 48.60 and 49.02 Rockwell C. According to FEA, the axe will not extensively fail during a worst-case scenario testing scenario, such as striking an anvil. Thus, the axe design should be sufficiently strong yet ductile to withstand battlefield usage and not become dull from such use.

## References

- [1] E. Oakeshott, *European Weapons and Armour From the Renaissance to the Industrial Revolution*, Cambridge: The Lutterworth Press, 1980.
- [2] "Steel Founder's Society of America," Marketing Options LLC, 2025. [Online]. Available: <https://www.sfsa.org/subject-areas/castinsteel/>. [Accessed 6 October 2025].
- [3] I. F. o. R. C. a. R. C. S. International Committee of the Red Cross, "Standard products catalogue," SolidPepper, [Online]. Available: <https://itemscatalogue.redcross.int/relief-4/tools-and-hardware--27/agricultural-tools--2/axe--RAGRTOOLAXE1.aspx>.
- [4] H. S. M. A. A. R. A. N. a. A. R. A. Mehrabi, "Improvement of AISI 4340 steel properties by intermediate quenching – microstructure, mechanical properties, and fractography," *International Journal of Materials Research*, vol. 111, no. 9, pp. 711-779, 2020.
- [5] Logie Timber, "Ash," 2026. [Online]. Available: <https://logietimber.co.uk/wood-types/ash/>.
- [6] E. Meier, "European Ash," 2026. [Online]. Available: <https://www.wood-database.com/european-ash/>.
- [7] Design, Granta, "Granta EduPack," Ansys, Cambridge, UK, 2025.
- [8] D. E. Kretschmann, "Mechanical Properties of Wood," USDA, 2010.
- [9] American Society for Testing and Materials, "Standard Test Methods for Rockwell Hardness of Metallic Materials," 02 October 2025. [Online]. Available: <https://compass.astm.org/content-access?contentCode=ASTM%7CE0018-25%7Cen-US>. [Accessed 25 March 2026].
- [10] X. Lan, "Science Direct," 1 September 2001. [Online]. Available: <https://www.sciencedirect.com/science/article/pii/S0017931001000059>.

## Appendix: Pictures and Figures

### Concept Generation



Figure 1. One of three concepts from the concept selection. This concept was rejected based upon the curved rear spike being prone to casting defects.

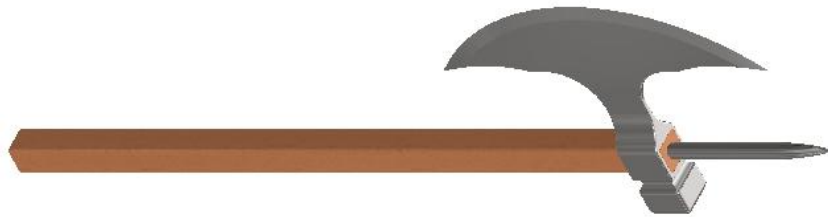


Figure 2. Two of three concepts from the concept selection. This concept was rejected as it does not take advantage of casting allowing for the head to be one piece.

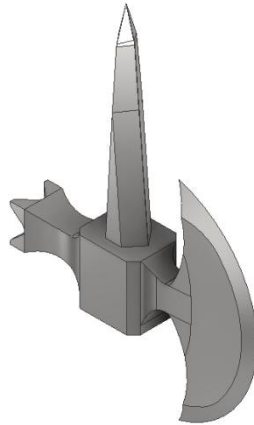


Figure 3. The final and chosen concept from concept selection. This concept was chosen due to its casting friendly geometry and its utilization of the benefits of casting over forging.

**Design Revision**



Figure 4. Isometric view of the revised axe head design.



Figure 5. Isometric view of the revised axe haft design.



Figure 6. Isometric view of the full axe design.

**Finite Element Analysis (FEA)**

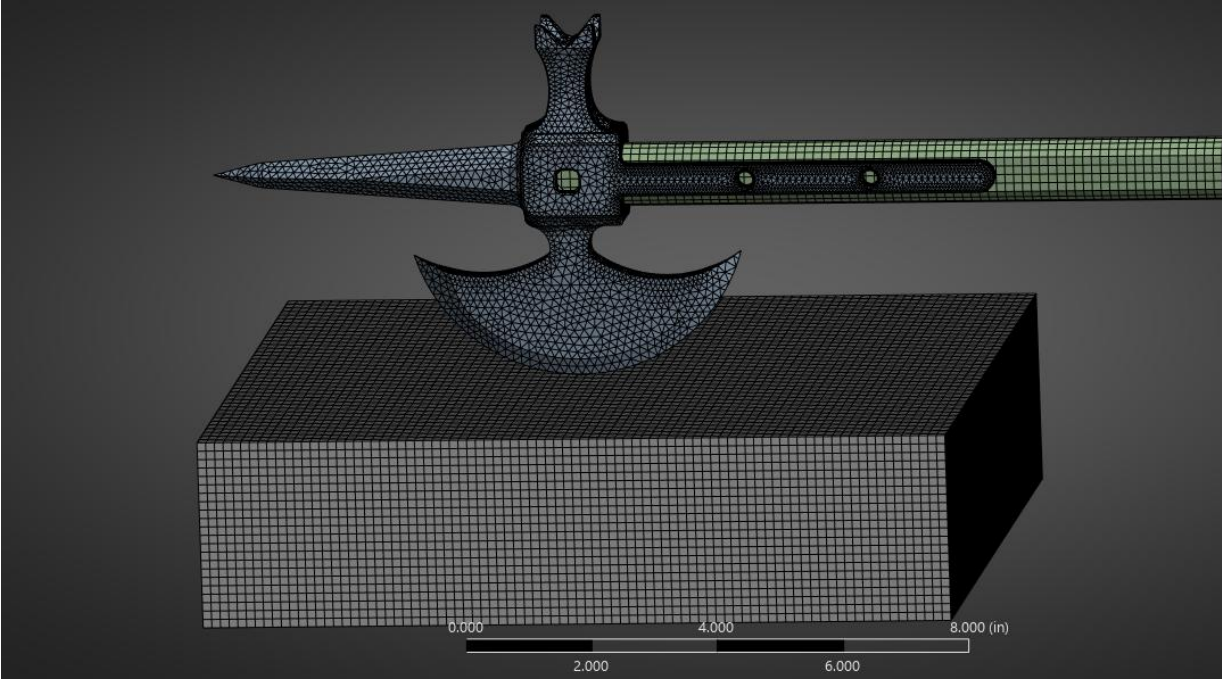


Figure 7. The final meshed model in Ansys including the axe head, handle and anvil-like block.

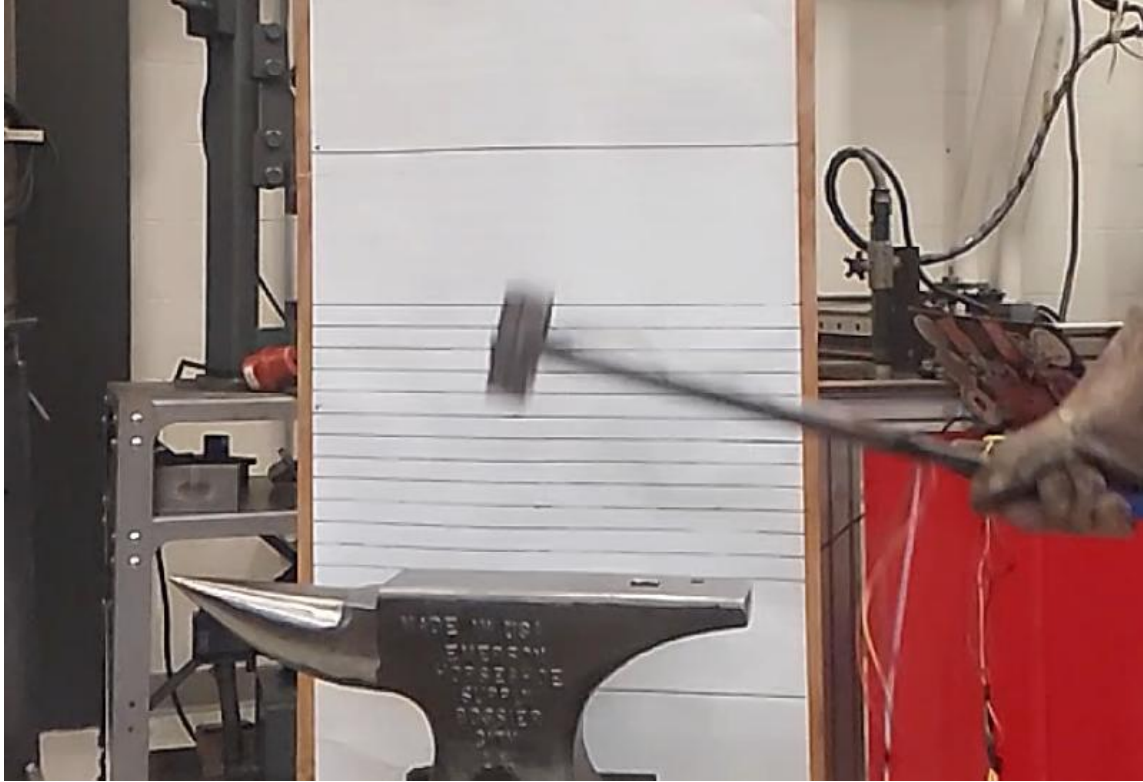


Figure 8. Mockup hammer setup to determine swinging speed.

Table 1. Mesh Convergence for the axe blade's explicit dynamics FEA model.

| Mesh Number | Mesh & Notes                                      | Mesh Statistics |                |           | Stress Convergence |           | Displacement Convergence |           | Acceptable? | Notes                               |
|-------------|---|-----------------|----------------|-----------|--------------------|-----------|--------------------------|-----------|-------------|-------------------------------------|
|             |   | Node Count:     | Element Count: | % Change: | Max [psi]:         | % Change: | Max [in]:                | % Change: |             |                                     |
| 1           | 0.31in Global Element Size, 0.5in Anvil           | 7879            | 12744          | N/A       | 209130             | N/A       | 0.047566                 | N/A       | N/A         |                                     |
| 2           | 0.265 in Global Element Size, 0.5in Anvil         | 8480            | 14723          | 15.53%    | 211220             | 1.00%     | 0.04776                  | 0.41%     | YES         |                                     |
| 3           | 0.24 in Global Element Size, 0.5in Anvil          | 9472            | 17398          | 18.17%    | 221220             | 4.73%     | 0.047705                 | 0.12%     | YES         |                                     |
| 4           | 0.1501in Global Element Size, 0.08in on Fillets   | 153751          | 171058         | 883.20%   | 199060             | 10.02%    | 0.047031                 | 1.41%     | No          |                                     |
| 5           | Same mesh at 4, @ 0.00005 seconds                 | 153751          | 171058         | 0.00%     | 219200             | 10.12%    | 0.025557                 | 45.66%    | N/A         | Changed to max stress at 0.00005sec |
| 6           | 0.1396in Global Element Size, 0.0501in on Fillets | 196449          | 232000         | 35.63%    | 226910             | 3.52%     | 0.025572                 | 0.06%     | YES         |                                     |
| 7           |   |                 |                |           |                    |           |                          |           |             |                                     |
| 8           |   |                 |                |           |                    |           |                          |           |             |                                     |

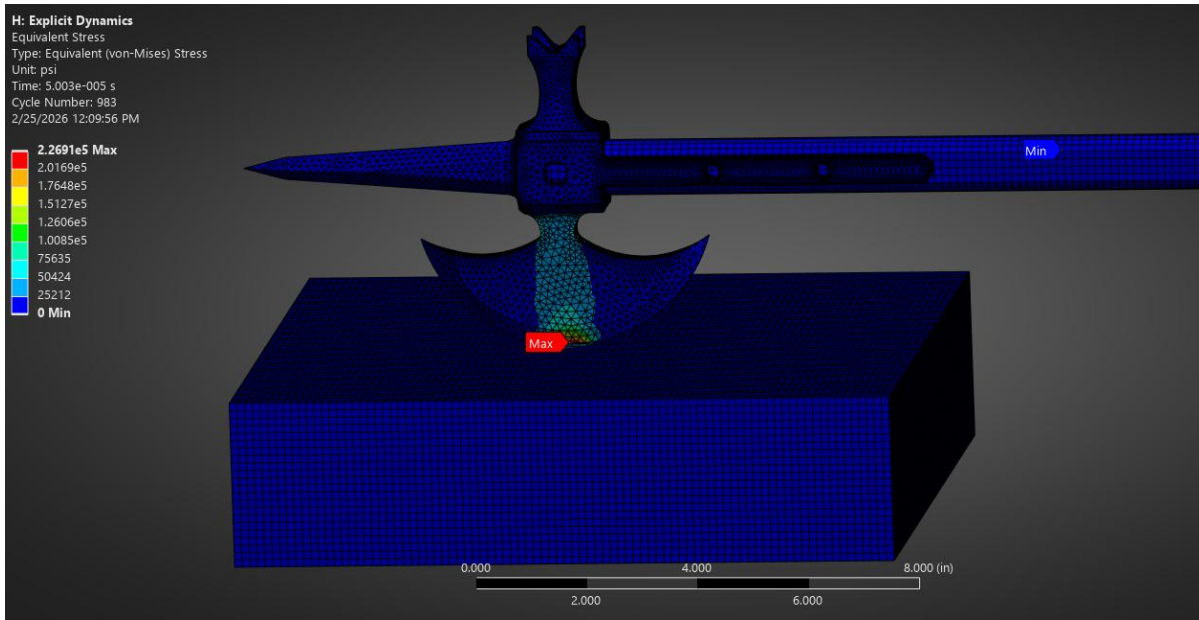


Figure 9. Von Mises Stress of the Axe-Block System.

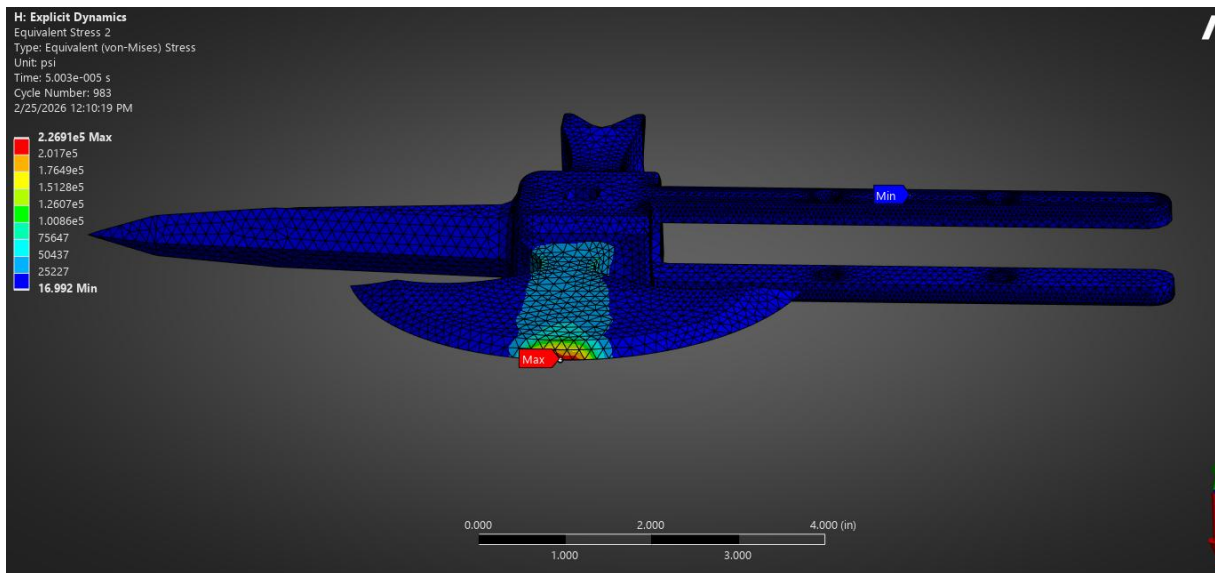


Figure 10. Zoomed in view of the Von Mises Stress of the Axe.

# Mold Design

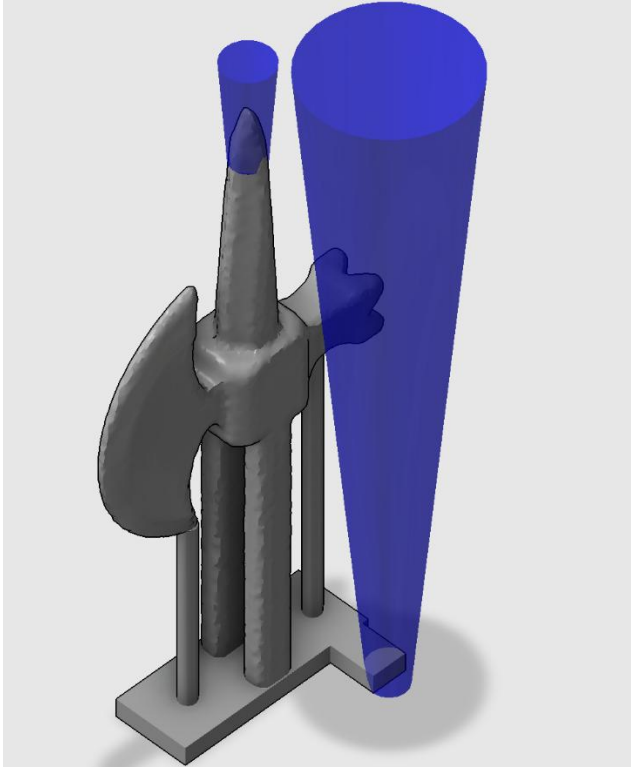


Figure 11. Isometric View of Mold 1.

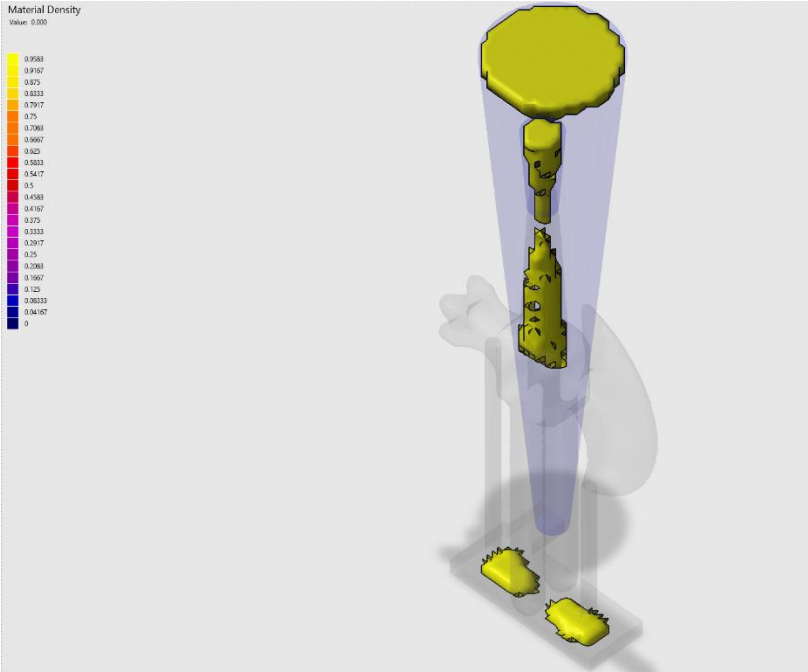


Figure 12. Iso-surface plot of material density for Mold 1.

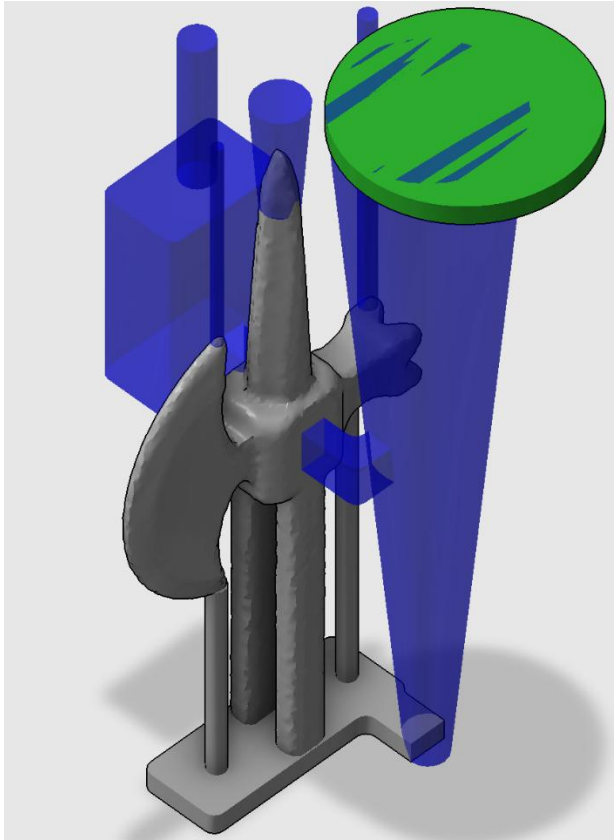


Figure 13. Isometric view of Mold 1.6.

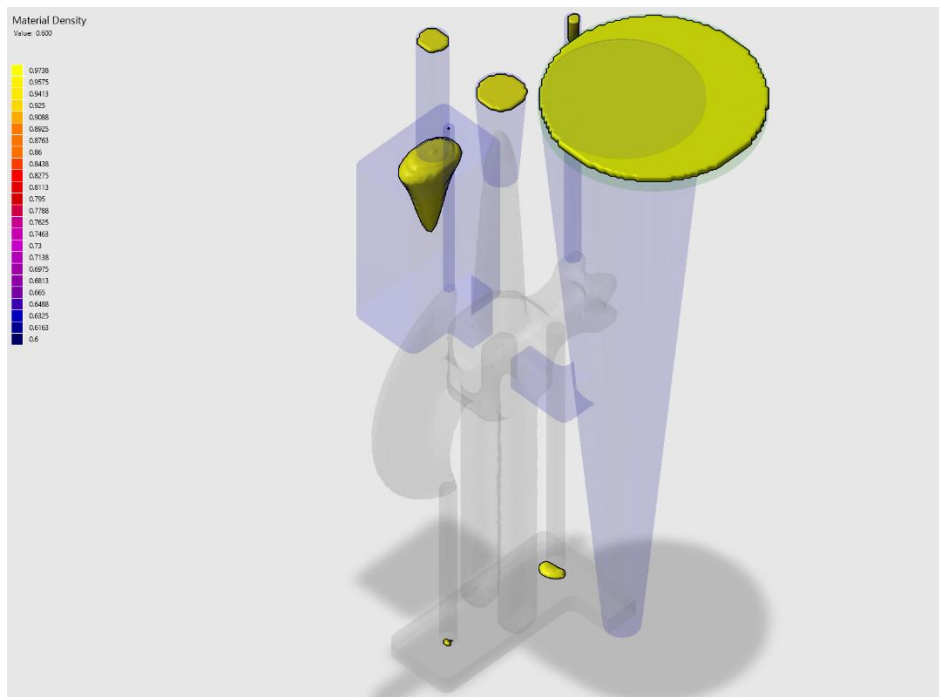


Figure 14. Iso-surface view of material density for Mold 1.6.

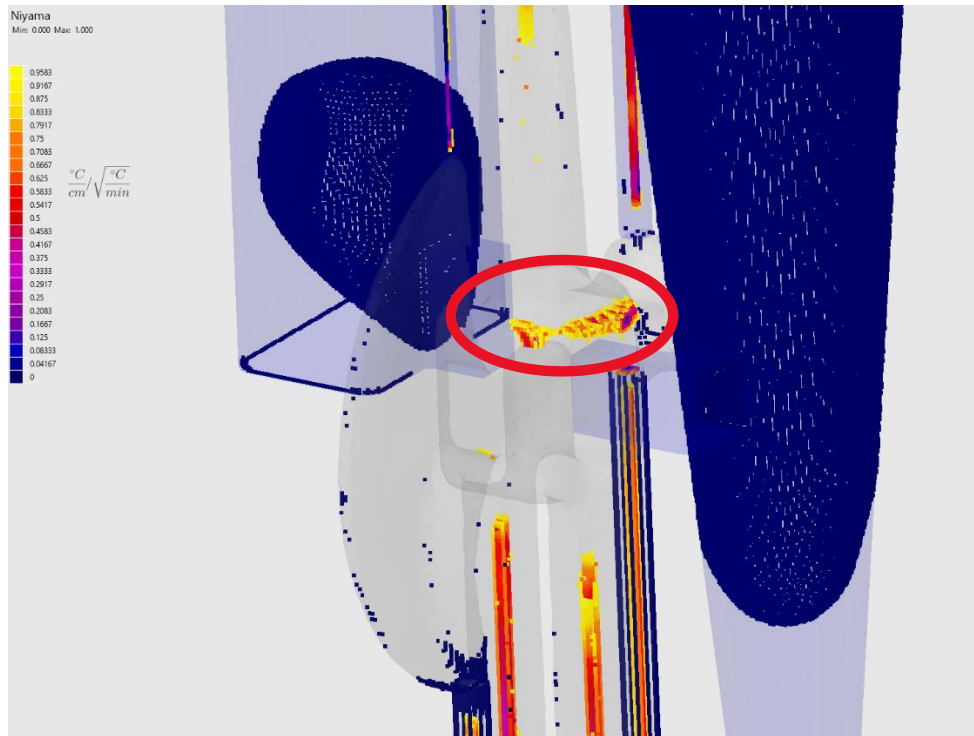


Figure 15. Iso-surface view of Niyama criterion for Mold 1.6.



Figure 16. Hot tearing on test pour of Mold 1.6.

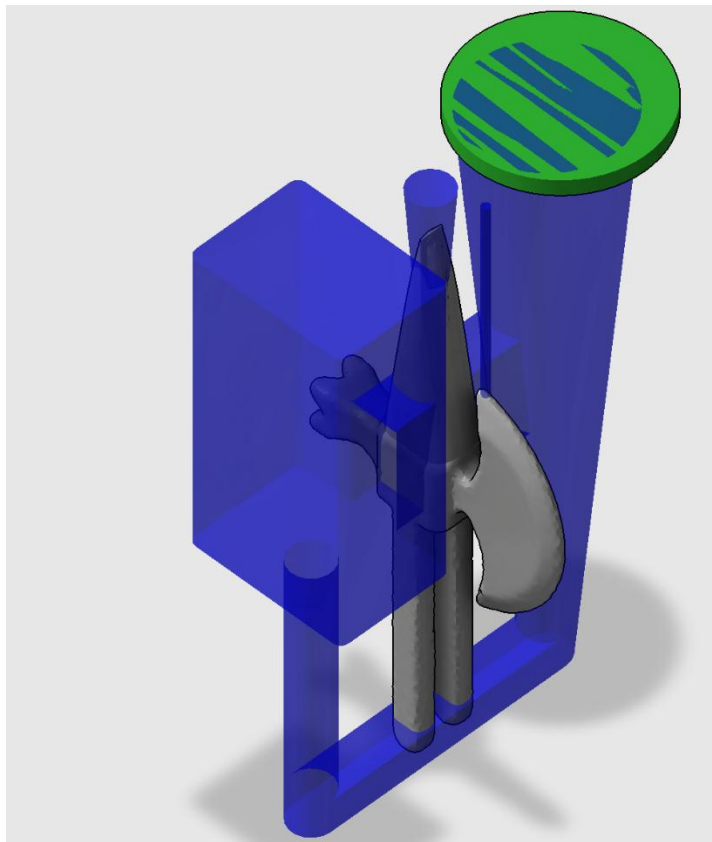


Figure 17. Isometric view of Mold 2.9.

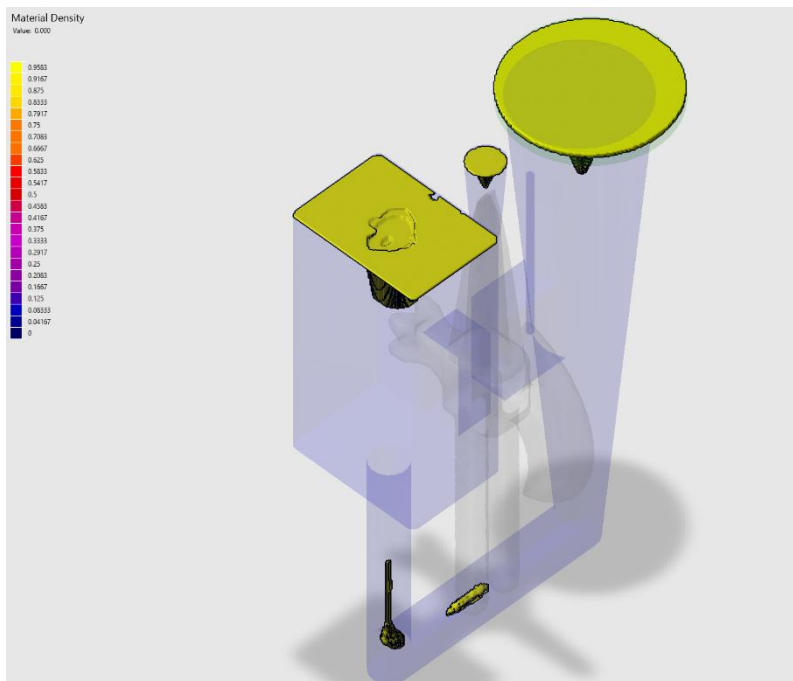


Figure 18. Iso-surface view of material density for Mold 2.9.

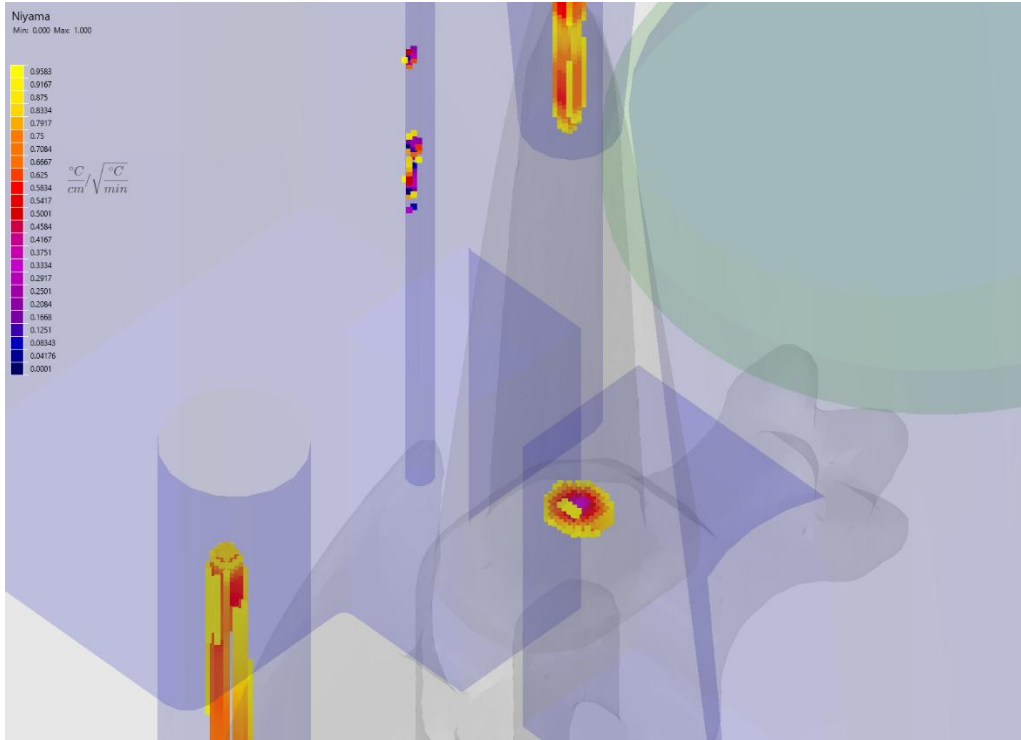


Figure 19. Iso-surface view of Niyama Criterion for Mold 2.9.

## Haft Carving



Figure 20. The haft being turned on a lathe.



Figure 21. The haft after being shaped by the belt sander, and ready for final sanding and fit.

# Machining, Heat Treatment, and Finishing



Figure 22. Raw casting from Mold 2.9.



Figure 23. Casting that had gating removed and a flat surface established for datum surface creation.

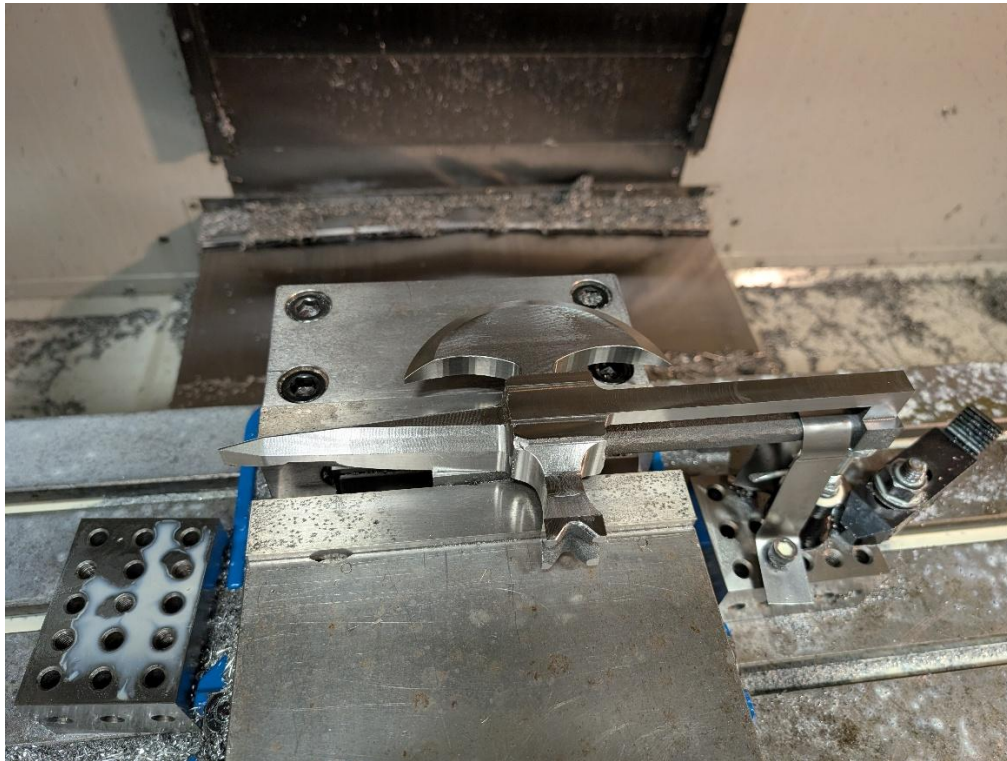


Figure 24. First side of the casting was rough machined.



Figure 25. The machined axe immediately after quenching and tempering.



Figure 26. Axe with ground edges in the middle of polishing.



Figure 27. Axe after polishing before assembly.

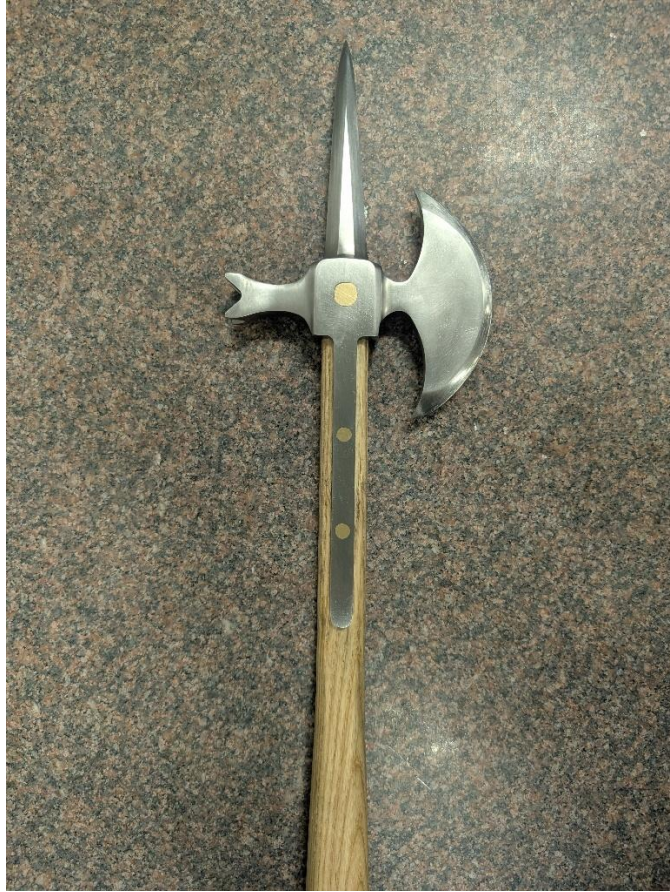


Figure 28. Fully finished and assembled Axe.